ISSN 0915-6313

NIFS--462

JP9704032

NATIONAL INSTITUTE FOR FUSION SCIENCE

Simulation Study on Cross Polarization Scattering of Ultrashort-Pulse Electromagnetic Waves

N. Katsuragawa, H. Hojo and A. Mase

(Received - Oct. 28, 1996)

NIFS-462 Nov. 1996

RESEARCH REPORT
NIFS Series

NAGOYA, JAPAN

Simulation Study on Cross Polarization Scattering of Ultrashort-Pulse Electromagnetic Waves

Naoki KATSURAGAWA, Hitoshi HOJO and Atushi MASE

Plasma Research Center, University of Tsukuba, Tsukuba 305

KEYWORDS: cross polarization scattering, ultrashort-pulse microwave, plasma diagnostic, magnetic fluctuation, Bragg resonance

Abstract

Simulation study on cross polarization scattering of ultrashort-pulse electromagnetic waves due to magnetic fluctuations is presented. One-dimensional coupled wave equations for the ordinary and extraordinary modes are solved for incident unipolar sub-cycle pulses in an inhomogeneous magnetized plasma. It is shown that the peak frequencies in the frequency-spectral signals of the mode-converted reflected waves are determined from the Bragg resonance condition in the wave numbers of the ordinary mode, the extraordinary mode and the magnetic fluctuations for relatively short-wavelength localized magnetic fluctuations.

Microwave-based diagnostics such as reflectometry are receiving recent growing attentions as a nonperturbing diagnostic for probing density profiles and fluctuations in magnetically confined plasmas.[1-5] In the tandem mirror GAMMA10, reflectometry with both the ordinary (O) and extraordinary (X) modes has been applied and the density and magnetic field fluctuations of the Alfvén ion cyclotron modes were observed.[1-3] More recently, cross polarization scattering phenomena of microwaves were observed in GAMMA10[6] and the Tore Supra tokamak.[7] Since the cross polarization scattering from the O to X mode or the X to O mode is caused by magnetic field fluctuations, it is of importance for probing magnetic fluctuations in magnetically confined plasmas.

In this Letter, we study numerically the cross polarization scattering of electromagnetic waves due to magnetic fluctuations in a magnetized cold plasma and discuss its diagnostic application for probing the magnetic fluctuations. For incident pulses, we assume unipolar sub-cycle pulses like as ultrashort-pulse reflectometry.[8-10] As an unipolar sub-cycle pulse can be considered as a set of many monochromatic plane waves with different frequencies, it possesses an advantage that the reflected or transmitted waves can carry a lot of information on fluctuations in a plasma as compared with the case of a monochromatic incident wave.

We consider electromagnetic waves (the O and X modes) propagating perpendicular to an constant external magnetic field $\boldsymbol{B}_0 (= B_0 \boldsymbol{e}_z, \boldsymbol{e}_z$ being the unit vector in the z-direction). The linearized wave equations describing the O and X modes are given by

$$(\frac{\partial^2}{\partial t^2} + c^2 \nabla \times \nabla \times) \boldsymbol{E} + \frac{1}{\epsilon_0} \frac{\partial}{\partial t} \boldsymbol{J} = 0 \qquad (1)$$

$$\frac{1}{\epsilon_0}\frac{\partial}{\partial t}\boldsymbol{J} = \omega_{pe}^2\boldsymbol{E} - \frac{1}{\epsilon_0}|\omega_{ce}|\boldsymbol{J}\times(\boldsymbol{e}_z + \frac{\tilde{\boldsymbol{B}}}{B_0}) \tag{2}$$

where $\boldsymbol{E}$ is the electric wave field, $\boldsymbol{J}$ is the current density, $\omega_{pe}(=\sqrt{e^2n_0/m_e\epsilon_0})$ the electron plasma frequency, $\omega_{ce}(=-eB_0/m_e)$ the electron cyclotron frequency, $-e$ the charge of the electron, m_e the electron mass, n_0 the plasma density and ϵ_0 the permittivity of vacuum. In the derivation of eq.(2), we assumed that the current density is approximated as $\boldsymbol{J} = -en_0\boldsymbol{v}_e$, $\boldsymbol{v}_e$ being the electron flow velocity, as we consider the electromagnetic waves in GHz range. Here $\tilde{\boldsymbol{B}}$ denotes the low-frequency magnetic fluctuations that are assumed to be static and $\tilde{\boldsymbol{B}} = \tilde{B}\boldsymbol{e}_y$ is also assumed. As the electromagnetic waves are in GHz range, the fluctuations in MHz or the lower-frequency range can be treated as static. We here neglect the effect of the density fluctuations associated with magnetic fluctuations for simplicity. We see that the Lorentz force term $\boldsymbol{J}\times\tilde{\boldsymbol{B}}$ in eq.(2) expresses the cross polarization scattering of electromagnetic waves due to magnetic fluctuations.

We here restrict ourselves to study one-dimensional wave propagation in the x-direction. We assume a Gaussian density profile given by $n_0(x) = N_0\exp(-x^2/L^2)$. In the numerical computation, we assumed $N_0 = 3\times10^{12}\mathrm{cm}^3$ ($\omega_{pe}(0)/2\pi \simeq 15.6\mathrm{GHz}$), $L = 20\mathrm{cm}$ and $|\omega_{ce}| = \omega_{pe}(x=0)$. We show the configuration for the present model in Fig.1, where the profiles of the right-hand cutoff ω_R (dashed line), the upper-hybrid frequency ω_{UH} (dotted line), ω_{pe} (solid line) and the left-hand cutoff ω_L (chain line) are shown. In the present configuration, E_z expresses the O mode and E_x and E_y correspond to the X mode. We here consider an unipolar O-mode pulse located at $x = x_0$ as the incident pulse at $t = 0$. The waveform of the incident pulse is assumed to be a Gaussian profile given by $E_z(x, t=0) = E_0\exp[-(x-x_0)^2/L_P^2]$ with L_P=0.5cm and $x_0 = -60\mathrm{cm}$. In this case, the

pulse width $\tau_p (= 2L_P/c$, c being the speed of light) is about 33ps and $1/\tau_p$ exceeds the maximum of $\omega_R/2\pi$. The incident pulse is also shown by a solid line in Fig.1. The waveform of the magnetic fluctuations is given by $\tilde{B}(x) = B_f \exp[-(x - x_B)^2/L_B^2] \sin[k_B(x - x_B)]$ where the parameters L_B, k_B and x_B characterize the profile of the fluctuation. We solve eqs.(1) and (2) by using a finite difference scheme.

We now present the computational results of eqs.(1) and (2). We first consider a magnetic fluctuation with k_B=3cm^{-1}, L_B=2cm and $x_B = -10$cm. In Fig.2, we show the wave profile of the magnetic fluctuation by a dotted line. The magnetic fluctuation is localized in a relatively narrow region in the vicinity of $x_B = -10$cm. In the figure, we also show the density profile $n_0(x)$ by a dashed line and the wave profile ($E_y(x)$) of the X mode caused by the cross polarization scattering at t =4ns by a solid line. As the wave equations (1) and (2) are linear, the amplitude of the mode-converted X mode is proportional to the amplitude B_f of the magnetic fluctuations as well as the amplitude E_0 of the incident O-mode pulse. However, at present we are concerned with not the amplitude of the mode-converted wave but the structure of the frequency spectrum. In Fig.3, we show the frequency-spectral signal of the mode-converted X mode ($E_y(x)$) that is reflected and received at $x = -60$cm by using a fast Fourier transform(FFT). We see that the spectral signal consists of two frequency domains. The lower-frequency domain is located roughly from 10GHz to 15GHz and the higher one is located roughly from 20GHz to 24GHz. In order to seek the peak frequencies of the spectral signal more precisely, we show the frequency-spectral signal of the mode-converted X mode obtained by a maximum entropy method(MEM) in Fig.4. We see that the spectral signal by the MEM is more

sharply distributed than that by the FFT. From Fig.4, we find that the peak frequencies of the spectral signal are 12.4GHz and 22.5GHz.

We hereafter show that the spectral signal obtained in Fig.3 or 4 is caused by the cross polarization scattering based on the Bragg resonance condition with respect to the wave numbers among the O and X modes and the magnetic fluctuation. The local wave number k is a function of x and frequency ω, as the density is non-uniform, and the wave number k_{fl} of the magnetic fluctuation is approximately given by $k_{fl} = k_B$. Let us assume that the cross polarization scattering from the O to X mode takes place at $x_B = -10$cm. There exist two types of the cross polarization scattering from the O to X mode. That is, one is the forward scattering and the other is the backward scattering. If we assume that the first peak of the spectral signal in Fig.4 is due to the backward scattering with the Bragg resonance condition of $k_O(\omega_1, x_B) - k_{fl} = -k_X(\omega_1, x_B)$, we obtain $\omega_1/2\pi$=12.3GHz from this Bragg condition. The value is very close to 12.4GHz obtained from Fig.4. Therefore, we conclude that the first peak of the spectral signal in Fig.4 is caused by the backward cross polarization scattering with the Bragg resonance condition of $k_O - k_{fl} = -k_X$. On the other hand, the second peak of the spectral signal in Fig.4 is supposed to be due to the forward scattering with the Bragg resonance condition of $k_O(\omega_2, x_B) - k_{fl} = k_X(\omega_2, x_B)$ and we obtain $\omega_2/2\pi$=22.3GHz. This value is also very close to 22.5GHz obtained from Fig.4. In this case, the forward-scattered X mode is reflected by the right-hand cutoff ω_R. Therefore, we also conclude that the second peak of the spectral in Fig.4 is caused by the forward cross polarization scattering with the Bragg resonance condition of $k_O - k_{fl} = k_X$.

We here note that the above arguments concerning with the cross polarization scat-

tering from the O to X mode can be easily explained by Fig.5, which determines the relationship between the frequencies ω of the mode-converted waves and the wave number k_{fl} of the magnetic fluctuation. In Fig.5, $k_O(\omega, x_B) + k_X(\omega, x_B)$ is expressed by solid lines, $k_O(\omega, x_B) - k_X(\omega, x_B)$ by a dashed line and $k_X(\omega, x_B) - k_O(\omega, x_B)$ by a chain line. As we have two branches for the X mode in the present plasma model, we see that there exist generally four processes in the cross polarization scattering for a given k_{fl}. From the figure, we see that at most of three processes can take place in the cross polarization scattering. In the case of $k_{fl} = k_B = 3\text{cm}^{-1}$ shown in Fig.2, though we have the third solution ω=18.2GHz in addition to $\omega/2\pi$=12.3GHz and 22.3GHz, however, we find that the spectral signal of the mode-converted X mode does not exist near $\omega/2\pi$=18.2GHz as shown in Fig.3 and 4. This is because the mode-converted X mode with $\omega/2\pi$=18.2GHz is a forward scattered wave and is almost absorbed at the upper-hybrid resonance ω_{UH} (In this case, there occurs no reflection of the X mode at the upper-hybrid resonance[11] and the transmission coefficient of the X mode crossing the upper-hybrid resonance is very small as $k_X\Delta >> 1$, Δ being the distance between the upper-hybrid resonance and the right-hand cutoff[11].) The hatched region shown in Fig.5 denotes the evanescent region (between ω_{UH} and ω_R) of the X mode. Therefore, we see that the mode-converted X mode with ω=18.2GHz is never observed at $x = x_0$.

To make clear the above arguments, we next calculate the case of $k_{fl} = k_B = 9\text{cm}^{-1}$, $L_B = 2$cm and $x_B = -10$cm. From Fig.5, we suppose that in this case only one solution with $\omega/2\pi = 26.0$GHz among three solutions in the mode-converted X modes can be observed in the reflected-wave signal, and that other two solutions are almost absorbed

at the upper-hybrid resonance ω_{UH} and are not observed. In Fig.6, we show that the frequency-spectral signal of the mode-converted X modes received at $x = x_0$ by the MEM for the case of k_B =9cm^{-1} with L_B =2cm and $x_B = -10$cm. We find only one peak in the spectral signal of the reflected X mode as we already expected, and the peak frequency is $\omega/2\pi$ =25.7GHz. We see that it is very close to $\omega/2\pi$ =26.0GHz estimated from Fig.5 under the assumption of $k_{fl} = k_B$.

As the conclusion, we can say that the peak frequencies in the spectral signals of the mode-converted waves are determined from the Bragg resonance condition in the wave numbers among the O and X modes and the magnetic fluctuations for relatively short-wavelength localized magnetic fluctuations. However, for a case of long-wavelength global magnetic fluctuations, we find that the spectral signal of the mode-converted wave are seemed to be insensitive to the Bragg resonance condition in the wave number. In Fig.7, we show the wave profile ($E_y(x)$, solid line) of the X mode converted from the O mode at t = 4ns for the case of k_B = 0.3cm^{-1}, L_B =20cm and x_B=0cm. In the figure, the density profile $n_0(x)$ (dashed line) and the wave profile of the magnetic fluctuation (dotted line) are also shown. In Fig.8, we show the frequency-spectral signal of the mode-converted reflected X mode received at $x = x_0$ by the FFT. In this case, we see that the spectral signal of the reflected X modes exists continuously up to 25GHz and we cannot find any sharp peaks in the spectral signal. (In this case, the MEM is also failed to yield any plausible results.) One reason for this is that the position at which the cross polarization scattering takes place does not become definite as the magnetic fluctuation is global.

Finally, we performed the simulation study on cross polarization scattering of ultrashort-

pulse electromagnetic waves due to magnetic fluctuations. We solved one-dimensional coupled wave equations for the O and X modes in an inhomogeneous cold plasma and investigated the cross polarization scattering process from the O to X modes due to magnetic fluctuations for incident sub-cycle O-mode pulses. We showed that the peak frequencies in the frequency-spectral signals of the mode-converted waves are determined from the Bragg resonance condition in the wave numbers among the O and X modes and the magnetic fluctuations for relatively short wavelength localized magnetic fluctuations.

This work was performed under the collaborating program at the National Institute for Fusion Science and also partly supported by a Grant-in-Aid for Scientific Research from the Ministry of Education, Science, Sports and Culture.

References

1) A. Mase, M. Ichimura, H. Satake, R. Katsumata, T. Tokuzawa, Y. Ito, H. Hojo, E. J. Doyle, A. Itakura, M. Inutake and T. Tamano : Phys. Fluids B5 (1993) 1677.

2) H. Hojo, A. Mase, M. Inutake and M. Ichimura : J. Plasma Fusion Res. **69** (1993) 1043.

3) A. Mase, H. Hojo, M. Kobayashi, N. Oyama, L. G. Bruskin, E. J. Doyle, T. Tokuzawa, A. Itakura, M. Ichimura and T. Tamano: *Diagnostics for Experimental Thermonuclear Fusion Reactors*, ed. P. Stott et al. (1996,Plenum) p.153.

4) C. Laviron, P. Millot and R. Prentice: Plasma Phys. Control. Fusion **37** (1995) 975.

5) M. Nagatsu: J. Plasma Fusion Res. **71** (1995) 132; references cited therein.

6) A. Mase, T. Tokuzawa, N. Oyama, Y. Ito, A. Itakura, H. Hojo, M. Ichimura and T. Tamano : Rev. Sci. Instrum. **66** (1995) 821.

7) X. L. Zou, L. Colas, M. Paume, J. M. Chareau, L. Laurent, P. Devynck and D. Gresillon: Phys. Rev. Lett. **75** (1995) 1090.

8) C. W. Domier, N. C. Luhmann, Jr., A. E. Chou, W. M. Zhang and A. J. Romanowski: Rev. Sci. Instrum. **66** (1995) 399.

9) B. I. Cohen, B. B. Afeyan, A. E. Chou and N. C. Luhmann, Jr.: Plasma Phys. Control. Fusion **37** (1995) 329.

10) N. Katsuragawa, H. Hojo, H. Honda and A. Mase : *Proc. 7th Int. Symp. Laser-Aided Plasma Diagnostics* (Dec. 1995, Fukuoka) p.345.

11) T. H. Stix: *The Theory of Plasma Waves* (McGraw-Hill,1962) Chap.10.

Figure Captions

Fig.1: The schematic view of the simulation model, where the profiles of the right-hand cutoff ω_R (dashed line), the upper-hybrid frequency ω_{UH} (dotted line), the electron plasma frequency ω_{pe} (solid line) and the left-hand cutoff ω_L (chain line) are shown. The incident O-mode pulse (solid line) is localized at $x = x_0 = -60$ cm.

Fig.2: The wave profile (E_y, solid line) of the X mode converted from the O-mode (E_z) by a localized magnetic fluctuation (dotted line) at t = 4ns, where k_B =3cm^{-1}, L_B =2cm and $x_B = -10$cm. The density profile (dashed line) is also shown.

Fig.3: The frequency-spectral signal of the mode-converted X mode (E_y) received at $x = -60$cm by the FFT for the localized magnetic fluctuation of Fig.2.

Fig.4: The frequency-spectral signal of the mode-converted X mode (E_y) by the MEM for the localized magnetic fluctuation of Fig.2. The two peak frequencies are $\omega/2\pi$ =12.4 and 22.5GHz.

Fig.5: The frequencies of the mode-converted X modes vs. the wave number of the magnetic fluctuation. For the Bragg resonance condition, $k_X + k_O$ (solid line), $k_O - k_X$ (dashed line) and $k_X - k_O$ (chain line) at $x = x_B = -10$cm are shown. The hatched region is the evanescent region of the X mode.

Fig.6: The frequency-spectral signal of the mode-converted X mode (E_y) by the MEM for the magnetic fluctuation with k_B =9cm^{-1}, L_B =2cm and $x_B = -10$cm. Only one peak frequency is observed at $\omega/2\pi$ = 25.7GHz.

Fig.7: The wave profile (E_y, solid line) of the X mode converted from the O-mode (E_z) by a global magnetic fluctuation (dotted line) at t =4ns, where k_B=0.3cm^{-1}, L_B=200cm and x_B=0cm.

Fig.8: The frequency-spectral signal of the mode-converted X mode (E_y) received at x = $-$60cm by the FFT for the global magnetic fluctuation of Fig.7.

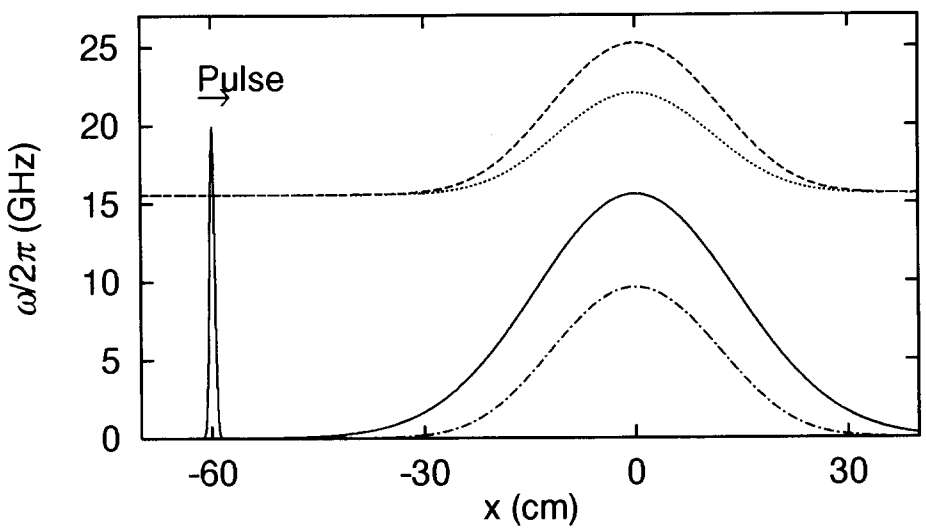

Fig.1

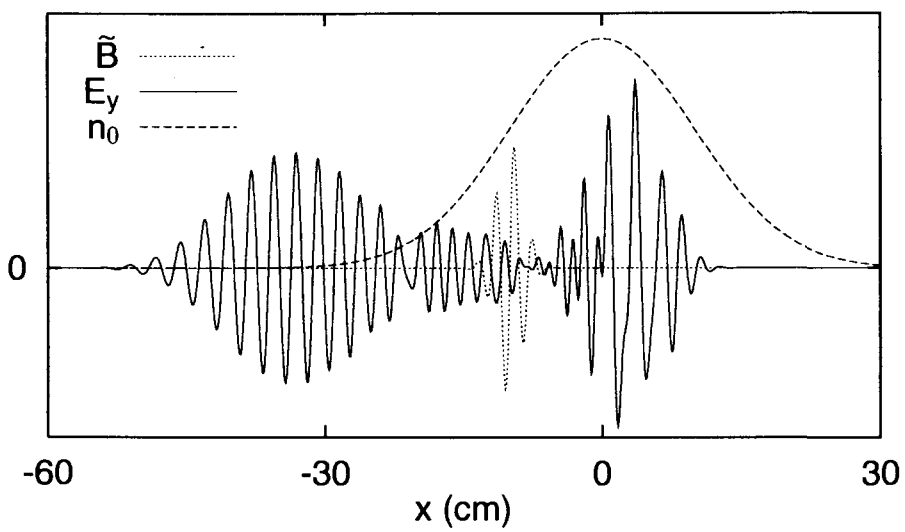

Fig.2

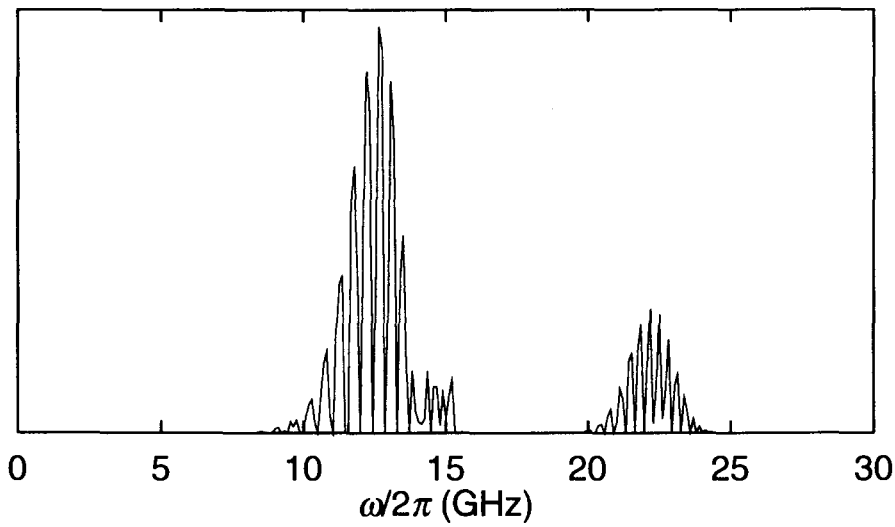

Fig.3

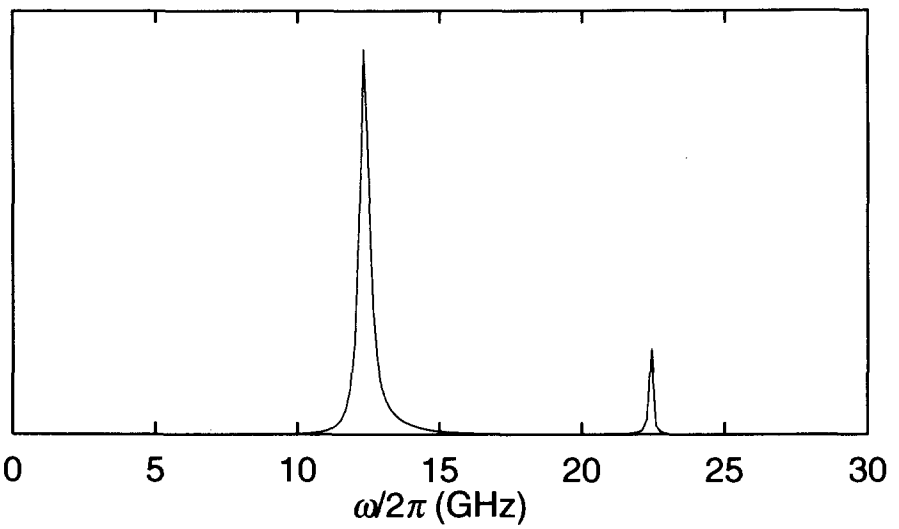

Fig.4

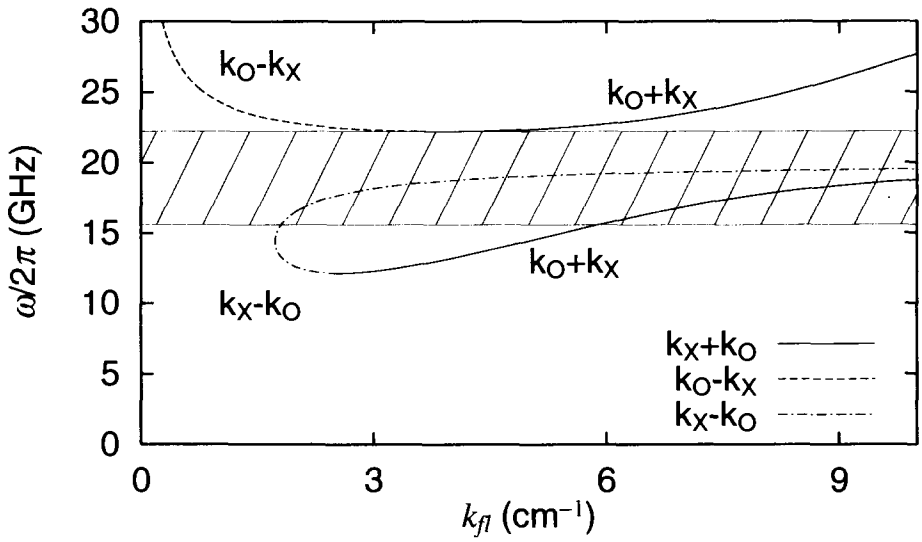
30
25
20
15
10
5
0
0
3
6
9
ω/2π (GHz)
k_fl (cm^-1)
k_O-k_X
k_O+k_X
k_O+k_X
k_X-k_O
k_X+k_O
k_O-k_X
k_X-k_O

Fig.5

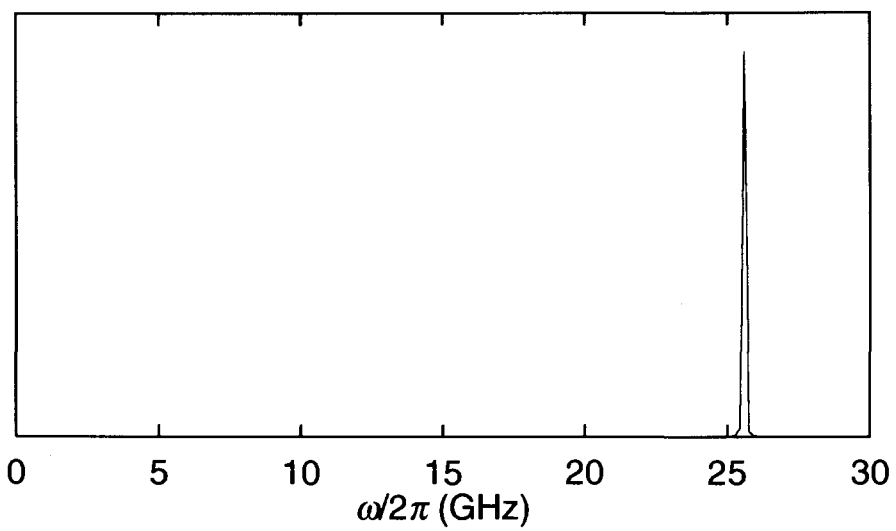

Fig.6

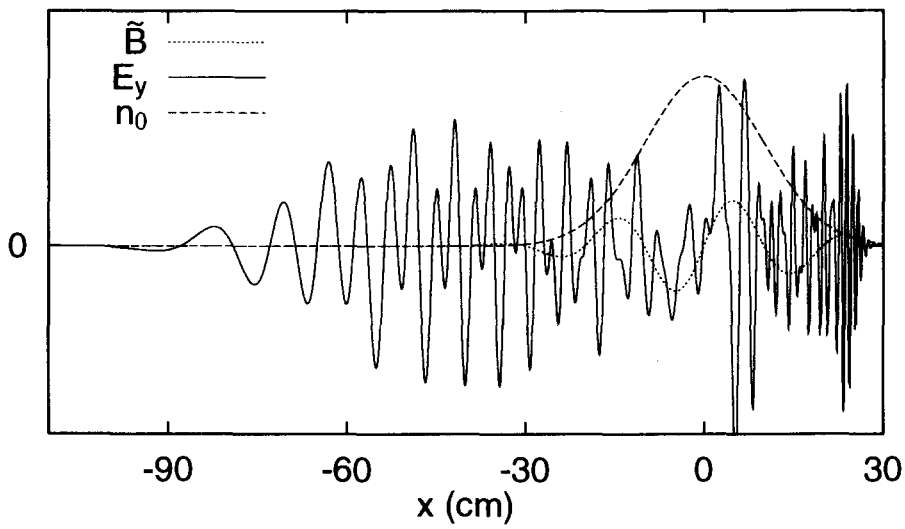

Fig.7

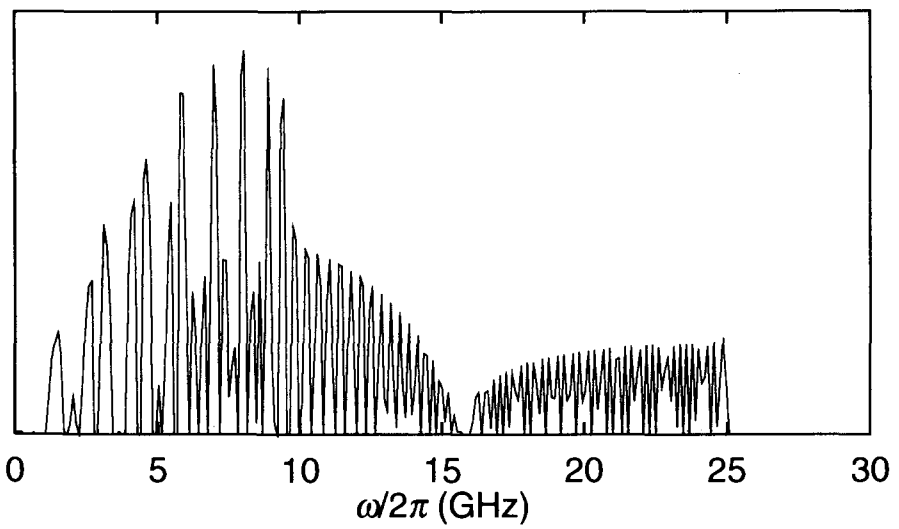

Fig.8

Recent Issues of NIFS Series

NIFS-424 K. Orito,
A New Technique Based on the Transformation of Variables for Nonlinear Drift and Rossby Vortices; July 1996

NIFS-425 A. Fujisawa, H. Iguchi, S. Lee, T.P. Crowley, Y. Hamada, H. Sanuki, K. Itoh, S. Kubo, H. Idei, T. Minami, K. Tanaka, K. Ida, S. Nishimura, S. Hidekuma, M. Kojima, C. Takahashi, S. Okamura and K. Matsuoka,
Direct Observation of Potential Profiles with a 200keV Heavy Ion Beam Probe and Evaluation of Loss Cone Structure in Toroidal Helical Plasmas on the Compact Helical System; July 1996

NIFS-426 H. Kitauchi, K. Araki and S. Kida,
Flow Structure of Thermal Convection in a Rotating Spherical Shell; July 1996

NIFS-427 S. Kida and S. Goto,
Lagrangian Direct-interaction Approximation for Homogeneous Isotropic Turbulence; July 1996

NIFS-428 V.Yu. Sergeev, K.V. Khlopenkov, B.V. Kuteev, S. Sudo, K. Kondo, F. Sano, H. Zushi, H. Okada, S. Besshou, T. Mizuuchi, K. Nagasaki, Y. Kurimoto and T. Obiki,
Recent Experiments on Li Pellet Injection into Heliotron E; Aug. 1996

NIFS-429 N. Noda, V. Philipps and R. Neu,
A Review of Recent Experiments on W and High Z Materials as Plasma-Facing Components in Magnetic Fusion Devices; Aug. 1996

NIFS-430 R.L. Tobler, A. Nishimura and J. Yamamoto,
Design-Relevant Mechanical Properties of 316-Type Stainless Steels for Superconducting Magnets; Aug. 1996

NIFS-431 K. Tsuzuki, M. Natsir, N. Inoue, A. Sagara, N. Noda, O. Motojima, T. Mochizuki, T. Hino and T. Yamashina,
Hydrogen Absorption Behavior into Boron Films by Glow Discharges in Hydrogen and Helium; Aug. 1996

NIFS-432 T.-H. Watanabe, T. Sato and T. Hayashi,
Magnetohydrodynamic Simulation on Co- and Counter-helicity Merging of Spheromaks and Driven Magnetic Reconnection; Aug. 1996

NIFS-433 R. Horiuchi and T. Sato,
Particle Simulation Study of Collisionless Driven Reconnection in a Sheared Magnetic Field; Aug. 1996

NIFS-434 Y. Suzuki, K. Kusano and K. Nishikawa,
Three-Dimensional Simulation Study of the Magnetohydrodynamic

Relaxation Process in the Solar Corona. II.; Aug. 1996

NIFS-435 H. Sugama and W. Horton,
Transport Processes and Entropy Production in Toroidally Rotating Plasmas with Electrostatic Turbulence; Aug. 1996

NIFS-436 T. Kato, E. Rachlew-Källne, P. Hörling and K.-D Zastrow,
Observations and Modelling of Line Intensity Ratios of OV Multiplet Lines for 2s3s 3S1 - 2s3p 3Pj; Aug. 1996

NIFS-437 T. Morisaki, A. Komori, R. Akiyama, H. Idei, H. Iguchi, N. Inoue, Y. Kawai, S. Kubo, S. Masuzaki, K. Matsuoka, T. Minami, S. Morita, N. Noda, N. Ohyabu, S. Okamura, M. Osakabe, H. Suzuki, K. Tanaka, C. Takahashi, H. Yamada, I. Yamada and O. Motojima,
Experimental Study of Edge Plasma Structure in Various Discharges on Compact Helical System; Aug. 1996

NIFS-438 A. Komori, N. Ohyabu, S. Masuzaki, T. Morisaki, H. Suzuki, C. Takahashi, S. Sakakibara, K. Watanabe, T. Watanabe, T. Minami, S. Morita, K. Tanaka, S. Ohdachi, S. Kubo, N. Inoue, H. Yamada, K. Nishimura, S. Okamura, K. Matsuoka, O. Motojima, M. Fujiwara, A. Iiyoshi, C. C. Klepper, J.F. Lyon, A.C. England, D.E. Greenwood, D.K. Lee, D.R. Overbey, J.A. Rome, D.E. Schechter and C.T. Wilson,
Edge Plasma Control by a Local Island Divertor in the Compact Helical System; Sep. 1996 (IAEA-CN-64/C1-2)

NIFS-439 K. Ida, K. Kondo, K. Nagaski T. Hamada, H. Zushi, S. Hidekuma, F. Sano, T. Mizuuchi, H. Okada, S. Besshou, H. Funaba, Y. Kurimoto, K. Watanabe and T. Obiki,
Dynamics of Ion Temperature in Heliotron-E; Sep. 1996 (IAEA-CN-64/CP-5)

NIFS-440 S. Morita, H. Idei, H. Iguchi, S. Kubo, K. Matsuoka, T. Minami, S. Okamura, T. Ozaki, K. Tanaka, K. Toi, R. Akiyama, A. Ejiri, A. Fujisawa, M. Fujiwara, M. Goto, K. Ida, N. Inoue, A. Komori, R. Kumazawa, S. Masuzaki, T. Morisaki, S. Muto, K. Narihara, K. Nishimura, I. Nomura, S. Ohdachi, M.. Osakabe, A. Sagara, Y. Shirai, H. Suzuki, C. Takahashi, K. Tsumori, T. Watari, H. Yamada and I. Yamada,
A Study on Density Profile and Density Limit of NBI Plasmas in CHS; Sep. 1996 (IAEA-CN-64/CP-3)

NIFS-441 O. Kaneko, Y. Takeiri, K. Tsumori, Y. Oka, M. Osakabe, R. Akiyama, T. Kawamoto, E. Asano and T. Kuroda,
Development of Negative-Ion-Based Neutral Beam Injector for the Large Helical Device; Sep. 1996 (IAEA-CN-64/GP-9)

NIFS-442 K. Toi, K.N. Sato, Y. Hamada, S. Ohdachi, H. Sakakita, A. Nishizawa, A. Ejiri, K. Narihara, H. Kuramoto, Y. Kawasumi, S. Kubo, T. Seki, K. Kitachi, J. Xu, K. Ida, K. Kawahata, I. Nomura, K. Adachi, R. Akiyama, A. Fujisawa, J. Fujita, N. Hiraki, S. Hidekuma, S. Hirokura, H. Idei, T. Ido, H. Iguchi, K. Iwasaki, M.

Isobe, O. Kaneko, Y. Kano, M. Kojima, J. Koog, R. Kumazawa, T. Kuroda, J. Li, R. Liang, T. Minami, S. Morita, K. Ohkubo, Y. Oka, S. Okajima, M. Osakabe, Y. Sakawa, M. Sasao, K. Sato, T. Shimpo, T. Shoji, H. Sugai, T. Watari, I. Yamada and K. Yamauti,
Studies of Perturbative Plasma Transport, Ice Pellet Ablation and Sawtooth Phenomena in the JIPP T-IIU Tokamak; Sep. 1996 (IAEA-CN-64/A6-5)

NIFS-443 Y. Todo, T. Sato and The Complexity Simulation Group,
Vlasov-MHD and Particle-MHD Simulations of the Toroidal Alfvén Eigenmode; Sep. 1996 (IAEA-CN-64/D2-3)

NIFS-444 A. Fujisawa, S. Kubo, H. Iguchi, H. Idei, T. Minami, H. Sanuki, K. Itoh, S. Okamura, K. Matsuoka, K. Tanaka, S. Lee, M. Kojima, T.P. Crowley, Y. Hamada, M. Iwase, H. Nagasaki, H. Suzuki, N. Inoue, R. Akiyama, M. Osakabe, S. Morita, C. Takahashi, S. Muto, A. Ejiri, K. Ida, S. Nishimura, K. Narihara, I. Yamada, K. Toi, S. Ohdachi, T. Ozaki, A. Komori, K. Nishimura, S. Hidekuma, K. Ohkubo, D.A. Rasmussen, J.B. Wilgen, M. Murakami, T. Watari and M. Fujiwara,
An Experimental Study of Plasma Confinement and Heating Efficiency through the Potential Profile Measurements with a Heavy Ion Beam Probe in the Compact Helical System; Sep. 1996 (IAEA-CN-64/C1-5)

NIFS-445 O. Motojima, N. Yanagi, S. Imagawa, K. Takahata, S. Yamada, A. Iwamoto, H. Chikaraishi, S. Kitagawa, R. Maekawa, S. Masuzaki, T. Mito, T. Morisaki, A. Nishimura, S. Sakakibara, S. Satoh, T. Satow, H. Tamura, S. Tanahashi, K. Watanabe, S. Yamaguchi, J. Yamamoto, M.Fujiwara and A. Iiyoshi,
Superconducting Magnet Design and Construction of LHD; Sep. 1996 (IAEA-CN-64/G2-4)

NIFS-446 S. Murakami, N. Nakajima, S. Okamura, M. Okamoto and U. Gasparino,
Orbit Effects of Energetic Particles on the Reachable β–Value and the Radial Electric Field in NBI and ECR Heated Heliotron Plasmas; Sep. 1996 (IAEA-CN-64/CP -6) Sep. 1996

NIFS-447 K. Yamazaki, A. Sagara, O. Motojima, M. Fujiwara, T. Amano, H. Chikaraishi, S. Imagawa, T. Muroga, N. Noda, N. Ohyabu, T. Satow, J.F. Wang, K.Y. Watanabe, J. Yamamoto , H. Yamanishi, A. Kohyama, H. Matsui, O. Mitarai, T. Noda, A.A. Shishkin, S. Tanaka and T. Terai
Design Assessment of Heliotron Reactor; Sep. 1996 (IAEA-CN-64/G1-5)

NIFS-448 M. Ozaki, T. Sato and the Complexity Simulation Group,
Interactions of Convecting Magnetic Loops and Arcades; Sep. 1996

NIFS-449 T. Aoki,
Interpolated Differential Operator (IDO) Scheme for Solving Partial Differential Equations; Sep. 1996

NIFS-450 D. Biskamp and T. Sato,
Partial Reconnection in the Sawtooth Collapse; Sep. 1996

NIFS-451 J. Li, X. Gong, L. Luo, F.X. Yin, N. Noda, B. Wan, W. Xu, X. Gao, F. Yin, J.G. Jiang, Z. Wu., J.Y. Zhao, M. Wu, S. Liu and Y. Han,
Effects of High Z Probe on Plasma Behavior in HT-6M Tokamak; Sep. 1996

NIFS-452 N. Nakajima, K. Ichiguchi, M. Okamoto and R.L. Dewar,
Ballooning Modes in Heliotrons/Torsatrons; Sep. 1996 (IAEA-CN-64/D3-6)

NIFS-453 A. Iiyoshi,
Overview of Helical Systems; Sep. 1996 (IAEA-CN-64/O1-7)

NIFS-454 S. Saito, Y. Nomura, K. Hirose and Y.H. Ichikawa,
Separatrix Reconnection and Periodic Orbit Annihilation in the Harper Map; Oct. 1996

NIFS-455 K. Ichiguchi, N. Nakajima and M. Okamoto,
Topics on MHD Equilibrium and Stability in Heliotron / Torsatron; Oct. 1996

NIFS-456 G. Kawahara, S. Kida, M. Tanaka and S. Yanase,
Wrap, Tilt and Stretch of Vorticity Lines around a Strong Straight Vortex Tube in a Simple Shear Flow; Oct. 1996

NIFS-457 K. Itoh, S.- I. Itoh, A. Fukuyama and M. Yagi,
Turbulent Transport and Structural Transition in Confined Plasmas; Oct. 1996

NIFS-458 A. Kageyama and T. Sato,
Generation Mechanism of a Dipole Field by a Magnetohydrodynamic Dynamo; Oct. 1996

NIFS-459 K. Araki, J. Mizushima and S. Yanase,
The Non-axisymmetric Instability of the Wide-Gap Spherical Couette Flow; Oct. 1996

NIFS-460 Y. Hamada, A. Fujisawa, H. Iguchi, A. Nishizawa and Y. Kawasumi,
A Tandem Parallel Plate Analyzer; Nov. 1996

NIFS-461 Y. Hamada, A. Nishizawa, Y. Kawasumi, A. Fujisawa, K. Narihara, K. Ida, A. Ejiri, S. Ohdachi, K. Kawahata, K. Toi, K. Sato, T. Seki, H. Iguchi, K. Adachi, S. Hidekuma, S.Hirokura, K. Iwasaki, T. Ido, M. Kojima, J. Koong, R. Kumazawa, H. Kuramoto, T. Minami, I. Nomura, H. Sakakita, M. Sasao, K.N. Sato, T. Tsuzuki, J. Xu, I. Yamada and T. Watari,
Density Fluctuation in JIPP T-IIU Tokamak Plasmas Measured by a Heavy Ion Beam Probe; Nov. 1996

NIFS-462 N. Katsuragawa, H. Hojo and A. Mase,
Simulation Study on Cross Polarization Scattering of Ultrashort-Pulse Electromagnetic Waves; Nov. 1996